Chapter 11
Femtosecond Time-Resolved Photoelectron Spectroscopy of Molecular Anions

Alice Kunin and Daniel M. Neumark

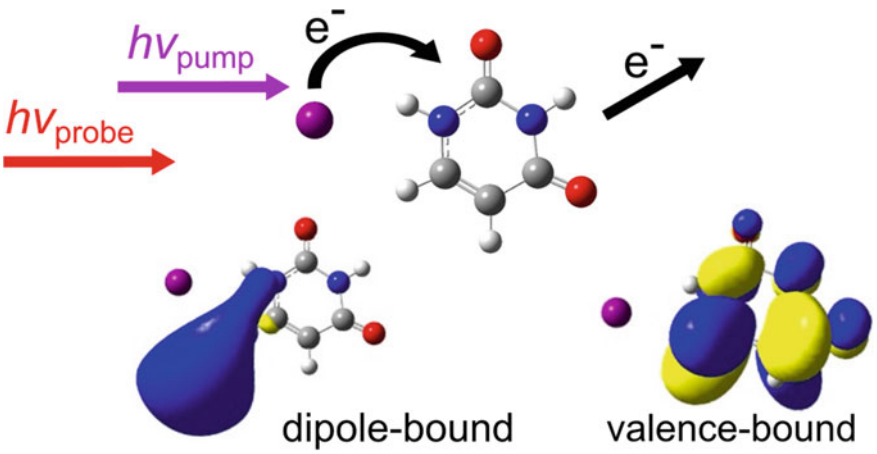

We explore the application of this technique to probe electron attachment and photodissociation dynamics in iodide–nucleobase clusters. The pump pulse initiates intracluster charge transfer, creating transient nucleobase anions that model DNA damage pathways induced by low-energy electron attachment. Image is reproduced from Ref. [57] with permission from the PCCP Owner Societies

T. Ebata and M. Fujii (eds.), *Physical Chemistry of Cold Gas-Phase Functional Molecules and Clusters*,
https://doi.org/10.1007/978-981-13-9371-6_11

Abstract Femtosecond time-resolved photoelectron spectroscopy (TRPES) is a powerful technique to probe the ultrafast excited state dynamics of molecules. TRPES applied to gas-phase molecular anions and clusters is capable of probing not only excited state formation and relaxation but also electron accommodation dynamics upon injection of an excess electron into a solvent or molecule. We review the basics of TRPES as it applies to molecular anions and several applications including the study of electron solvation dynamics in clusters and excited state relaxation in several biomolecules. We then explore in detail the dynamics of electron attachment and photodissociation in iodide–nucleobase clusters studied by TRPES as a model system for examining radiative damage of DNA induced by low-energy electrons. By initiating charge transfer from iodide to the nucleobase and following the dynamics of the resulting transient negative ions with femtosecond time resolution, TRPES provides a novel window into the chemistry triggered by the attachment of low-energy electrons to nucleobases.

Keywords Femtochemistry · Photodissociation · Photoexcitation · Nucleobases · Anion photoelectron spectroscopy

11.1 Introduction

Anions are ubiquitous in nature and are important in many biological processes and chemical phenomena. Anionic clusters, which are gas-phase size-selected aggregates of atoms or molecules with one or more excess electrons, can readily be mass-selected and hence are particularly useful model systems to study the evolution of electronic and vibrational structure as a function of size for many systems, including carbon clusters [1, 2], metal and semiconductor clusters [3–6], and solute–solvent clusters [7–9]. One can also investigate electron accommodation or solvation dynamics in an isolated environment [10, 11], thus gaining new insights into the energetics and mechanism of electron solvation in water and other solvents [12]. Anionic clusters can also model charge transfer processes such as charge-transfer-to-solvent (CTTS) transitions with the use of an anionic dopant that, upon photoexcitation, injects the excess electron into the solvent [12, 13]. Modeling electron transfer and attachment dynamics is especially relevant for the study of a number of biological processes such as single- and double-strand DNA damage induced by low-energy electron attachment [14], or dynamics in electron transport chains found in photosynthesis and cellular respiration processes [15].

A. Kunin · D. M. Neumark (✉)
Department of Chemistry, University of California, Berkeley, CA 94720, USA
e-mail: dneumark@berkeley.edu

A. Kunin
e-mail: alicekunin@berkeley.edu

D. M. Neumark
Lawrence Berkeley National Laboratory, Chemical Sciences Division, Berkeley, CA 94720, USA

Femtosecond (fs) time-resolved photoelectron spectroscopy (TRPES) is a powerful technique to probe the excited states and ultrafast relaxation or dissociation dynamics in molecules and clusters [16–18]. In anions, this pump–probe technique creates an excited state upon pump excitation of a ground state anion; the probe pulse photodetaches the excess electron and the resulting time-evolving photoelectron energy and angular distribution follow the relaxation or decay dynamics. Negative ions are particularly well-suited to study with TRPES as the excess electron binding energy is typically within the range of energies that can be easily generated by traditional Ti:Sapphire ultrafast lasers.

The basic principles and several applications of TRPES have been thoroughly reviewed [11, 15–28], so we focus here on only the key concepts as they relate to the study of anions. Single-photon anion photoelectron spectroscopy (PES) [29–35], shown schematically in Fig. 11.1a, employs a laser beam of photon energy hν to photodetach the excess electron of a prepared, stable anion. Only if the photon energy exceeds the electron binding energy (eBE) of the electron to the anion can the excess electron be detached. The kinetic energy (eKE) distribution of the outgoing photodetached electrons is measured, and the principle of energy conservation, as shown in Eq. 11.1, may then be used to determine accurate eBEs:

$$\mathrm{eBE} = h\nu - \mathrm{eKE} \tag{11.1}$$

For a one-electron transition, photodetachment can occur to any neutral vibrational (and electronic) states within the photon energy range, provided there is sufficient Franck–Condon overlap between the anion and neutral vibrational wavefunctions. Identification of the transition between the anion and neutral vibrational ground states

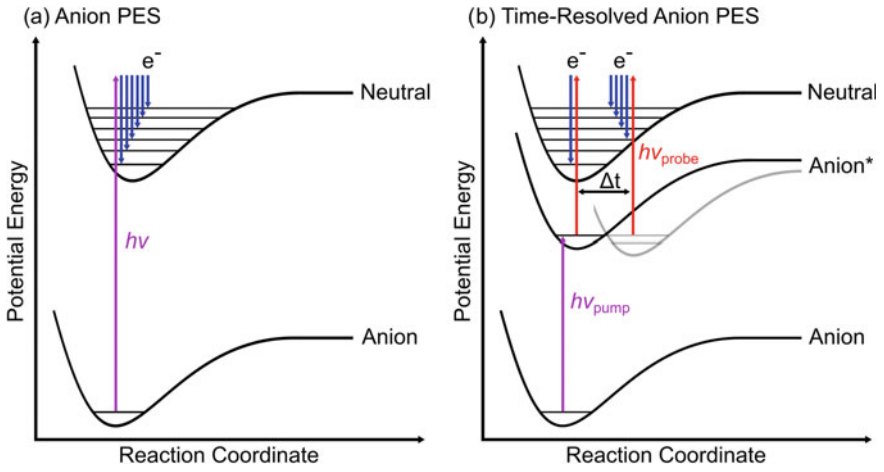

Fig. 11.1 Example scheme for **a** anion PES and **b** TRPES. Anion* indicates the photoexcited state. The blue lines indicate the resultant kinetic energies of the photodetached electrons. Reproduced from Ref. [57] with permission from the PCCP Owner Societies

yields the electron affinity (EA). The vertical detachment energy (VDE) corresponds to the difference in energy between the anion and the neutral at the equilibrium geometry of the anion. In spectra that do not show any vibrational structure, the VDE is identifiable as the peak or maximum intensity (maximum Franck–Condon overlap) of the photoelectron spectrum, and the width of the spectrum is an indication of the geometry change that occurs upon photodetachment.

Figure 11.1b shows a schematic diagram for fs anion TRPES. A fs pump pulse is used to generate an electronically excited anion, which can decay by multiple mechanisms including dissociation, internal conversion, or autodetachment. A time-delayed fs probe pulse photodetaches this transient negative ion (TNI) to monitor its temporal evolution, enabling characterization of these various pathways. A sufficiently energetic probe pulse can interrogate not only TNIs but also any anionic dissociation products that may form due to fragmentation, as well as radiationless transitions to other excited states or the anion ground state. The ability to follow ground state dynamics is a notable advantage of anion TRPES as compared to neutral TRPES, in which ionization from the ground state is often not energetically feasible. Thus, anion TRPES can offer a complete picture of the relaxation and dissociation dynamics subsequent to electronic excitation.

Anion TRPES has been previously applied to study size-dependent electron solvation dynamics or CTTS dynamics with an iodide dopant atom in a cluster of solvent molecules or atoms [12, 36]. Size-dependent relaxation dynamics have also been probed for carbon clusters [37, 38] and transition metal clusters [39–45] with anion TRPES. TRPES has also been applied to probe fundamental dynamics of long-range interactions involved in excess electron binding, such as non-valence-bound anionic states [46–48] and multiply charged anions (MCAs) [49–52]. In recent years, electronic resonances and electron accommodation dynamics in many biologically relevant species have been of great interest [53–57].

In this chapter, Sect. 11.2 provides a brief description of selected past studies to illustrate the nature of the information that is uniquely gained by the versatile application of TRPES to anionic clusters. Section 11.3 delves into the specific work that has been done in the Neumark group on the dynamics of TNI formation and decay in iodide–nucleobase ($I^-\cdot N$) clusters as a model system for the reductive damage of DNA. Section 11.4 covers the experimental and computational methodologies specific to the study of $I^-\cdot N$ complexes, and Sect. 11.5 examines the results of these TRPES studies of iodide–uracil ($I^-\cdot U$) and iodide–thymine ($I^-\cdot T$) clusters, as well as the simpler, model system of photoexcited iodide–nitromethane ($I^-\cdot CH_3NO_2$) clusters that provide an illustrative framework for understanding the more complex dynamics of the larger nucleobase species. We conclude with a summary and outlook for future applications of anion TRPES of iodide-containing clusters to advance our understanding of reductive damage pathways in DNA.

11.2 A Brief Overview of Past Anion TRPES Studies

Several TRPES studies by the Neumark and Zewail groups have been directed at probing relaxation dynamics in size-selected anionic clusters A_n^- and iodide-associated $I^-{\cdot}A_n$ clusters, including carbon clusters [37, 38, 58, 59], oxygen and solvated oxygen species [60–63], mercury [45, 64–67], and I_2^- and $I_2^-{\cdot}A_n$ [68–82], among others [83, 84]. Others have worked to theoretically simulate the TRPE spectra of I_2^- and $I_2^-{\cdot}Y$ complexes to aid and improve the dynamical analysis of these studies [85–88], and the I_2^- studies have also been extended by Sanov [89, 90] to probe the photodissociation dynamics of I_2Br^- and IBr^- anions. TRPES has also been used by the Eberhardt and Ganteför groups to explore dynamics of metal thermalization in transition metal A_n^- clusters [39–44, 91, 92] and desorption in metals with anionic adsorbates [93–98]. These transition metal cluster studies are able to probe the metal band structure and relaxation processes on a molecular level. Much of this work has been previously reviewed [11].

TRPES has been employed by Johnson [99], Neumark [100–104], and Zewail [36] to study size-selected $(H_2O)_n^-$ and $(D_2O)_n^-$ water clusters to probe the time-resolved dynamics of solvated electrons. These studies probed the excited state lifetimes of electronically excited water clusters as a model for the relaxation of the bulk solvated electron. The relaxation mechanism is expected to be initial relaxation along the excited state surface, internal conversion (IC), and finally ground state relaxation, but the timescales for each step are a matter of debate [12]. Transient absorption studies of hydrated electrons have measured a rapid, initial ~50 fs lifetime that has been ascribed either to relaxation along the excited state surface ("adiabatic" model) [105, 106] or IC ("nonadiabatic" model) [107] as the fastest observable step. TRPES of $(H_2O)_n^-$ clusters by Neumark and co-workers [101, 103, 108] measured abrupt appearance and decay of an excited state feature with concomitant dynamics for ground state depletion and recovery, which is indicative of decay by IC. A dramatic decrease in excited state lifetime was observed with increasing cluster size, with sub-100 fs IC of the excited state in the largest clusters studied (n = 70–200) [103]. Thus, this rapid timescale for IC strongly supports the nonadiabatic model for hydrated electron relaxation. This nonadiabatic mechanism is also more recently supported by TRPES studies of hydrated electrons in liquid microjets by Neumark [109, 110] and Suzuki [111].

TRPES of $I^-{\cdot}(H_2O)_n$ and $I^-{\cdot}(D_2O)_n$ clusters [112–114] allows one to study the injection of an excess electron into a solvent network as in a CTTS transition since a UV pump pulse can be used to promote charge transfer from the iodide to the solvent moiety (S_n), as in Eq. 11.2:

$$I^-{\cdot}S_n \xrightarrow{h\nu_{\text{pump}}} I\cdots S_n^{*-} \tag{11.2}$$

TRPES of $I^-{\cdot}(H_2O)_n$ most notably exhibited a strong shift to higher VDEs of the excited state feature after 1–2 ps, and greater magnitude shifting was observed in larger clusters. When compared to the VDEs measured for different isomers of

$(H_2O)_n^-$ clusters, this shift suggests that the water cluster relaxation proceeds in a few ps via isomerization from an initially surface bound excess electron to one that may be in a more tightly bound configuration [112–116].

Other S_n^- and $I^-{\cdot}S_n$ solvent clusters have also been investigated in time-resolved experiments by Neumark and Zewail, including those of methanol and various iodide–alcohol complexes [117–120], ammonia [121, 122], acetonitrile $(CH_3CN)_n^-$ [123, 124], and tetrahydrofuran (C_4H_8O) [125, 126]. Many of these solvents are suggested to share some similarities with the proposed relaxation schemes for water, although differences in hydrogen bonding and solvent molecule packing result in different sites or cavities that the excess electron can occupy. Additionally, the presence of different vibrational modes in these solvents compared to those of water affects the IC and solvent motion-driven relaxation pathways. These studies have been previously reviewed in considerable detail [11, 12].

Anion TRPES has also been employed to analyze the properties and dynamics of several nontraditional valence anions. While conventional anions have the excess electron occupying a valence orbital, non-valence-bound anions, in which there is a long-range attraction between the molecular core and the excess electron, are also important species [127]. These anions can be dipole-bound or multipole-bound if the neutral species possesses a sufficiently large dipole or multipole moment, as discussed in considerable detail in the later portions of this chapter. More recently, Verlet and co-workers have reported observation of correlation-bound states (CBSs) of the *para*-toluquinone trimer cluster anion $(pTQ)_3^-$ [47], and the iodide–hexafluorobenzene cluster ($I^-{\cdot}C_6F_6$) using TRPES [48]. Such CBSs have been described by calculations to be non-valence-bound states that arise from correlation forces between the excess electron and the molecular valence electrons [128–133]. With TRPES, the pump pulse is used to either excite the species to a π^* excited state that appears to internally convert to a transient CBS in <60 fs, as in the case of $(pTQ)_3^-$, or the pump pulse may generate the CBS directly via UV initiated charge transfer from iodide, as in $I^-{\cdot}C_6F_6$, and the probe pulse follows the evolution and decay of this metastable state.

Repulsive long-range interactions in the form of the repulsive Coulomb barrier (RCB) are fundamental in dictating the characteristics and stability of multiply charged anions (MCAs), as shown by Wang [33] and others [52]. For multiply charged anions with negative EA, the RCB can support (meta)stable gas-phase A^{n-} MCAs because although the energy of the excess electron may lie above the $A^{(n-1)-} + e^-$ energetic asymptote, the RCB imposes an energetic barrier such that this electron must be photoexcited well above the EA to be detached. TRPES has been used by Kappes [49–51, 134, 135] and Verlet [136–138] to probe the properties and decay dynamics of the resonant states that are bound by the RCB in a number of MCA fluorophores and chromophores. These time-resolved studies are able to determine the lifetimes for excited state IC, intersystem crossing, and tunneling autodetachment.

We close this section with a brief discussion of the more recent applications of TRPES to study a number of electron-driven processes prominent in biological systems. Electron transport chains (ETCs), for example, are key for energy extraction in photosynthesis and cellular respiration, and quinones are often found as electron

acceptors in ETCs [15]. TRPES has been used by Verlet to probe numerous anionic quinone derivatives [54, 139–142] including coenzyme Q_0 [143, 144] and vitamin K_3 [145] in a bottom-up approach to understanding the role of this structural motif in ETCs. Chemical substitutions in this class of quinones were used with TRPES to probe, for example, the effects of conjugation or various nearby electron-donating groups on the timescales and mechanisms of excited state IC. Important biological chromophores have also been studied with anion TRPES in the Verlet and Zewail groups, including stilbene [146], the anionic fluorescent chromophore of green fluorescent protein (GFP) [55, 147–149], and the timescales for twisting in the trans-to-cis isomerization process of the photoactive yellow protein chromophore [53].

Mechanisms of excited state relaxation and dissociation in DNA and its constituents are naturally of significant interest [150]. To this end, Verlet and co-workers have employed anion TRPES to study the excited state dynamics of isolated deprotonated DNA nucleotides [27, 56, 151]. These studies used UV pump energies near the nucleobase π-π^* transitions and probed the unique relaxation pathways and timescales for each nucleotide, deprotonated at the phosphate group, to model the non-radiative relaxation processes of DNA. Neumark and co-workers have examined dynamics in a number of iodide–nucleobase clusters, including iodide–uracil ($I^-{\cdot}U$) [152–155], iodide–thymine ($I^-{\cdot}T$) [153, 156], iodide–uracil–water [157], iodide–adenine [158], and the related system iodide–nitromethane ($I^-{\cdot}CH_3NO_2$) [46, 159], to elucidate the role of low-energy electron attachment to nucleobases in the mechanism of reductive damage of DNA. In the sections that follow, we cover in detail the ultrafast dynamics of electron attachment and photodissociation in photoexcited $I^-{\cdot}CH_3NO_2$, $I^-{\cdot}U$, and $I^-{\cdot}T$ clusters. This work is described in more detail elsewhere [57].

11.3 Application—Electron Attachment and Photodissociation Dynamics in I^-·Nucleobase Clusters

Low-energy electron attachment to DNA has been shown to induce damage such as single- and double-strand breaks, and the mechanism of this damage has been a topic of considerable interest in recent years [14]. The initial site of attachment has been implicated to be the DNA nucleobases, and upon attachment a TNI of the base is expected to form [160–162]. It is predicted that electron transfer from the base moiety to the sugar–phosphate backbone, facilitated by strong electronic coupling [160, 161, 163, 164], then leads to dissociation or fragmentation. These considerations have motivated many experimental and theoretical studies of the interactions between nucleic acid constituents and low-energy electrons [165].

A conventional valence-bound (VB) anion can be formed by electron attachment to the π^* orbital of the nucleobase [161, 166], but an excess electron can also be bound by the fairly large dipolar moment of the base to form a dipole-bound (DB)

anion [167]. A molecular dipole moment (μ) of at least ~2–2.5 D is needed to bind the excess electron; [168] all of the canonical nucleobase species examined here have larger dipole moments than this and are thus capable of forming DB anions [169–171]. Electron scattering experiments have suggested that the DB state is initially formed and may then convert or act as a "doorway" to the formation of a VB anion [172]. The decay of these metastable states is then expected to lead to dissociation or fragmentation of the nucleobases, the larger nucleotide, or the DNA backbone structure [173, 174]. To better understand the role of these nucleobase DB and VB anions in DNA damage, many laboratories have probed these anions with a variety of experimental techniques, including dissociative electron attachment [172, 175–177] and anion PES [166, 178, 179]. Numerous theoretical studies of these anions have been carried out as well [180–184]. Anion TRPES is uniquely able to probe the ultrafast time-resolved dynamics and evolution of these TNIs, including interconversion of a DB anion to form a VB anion, as well as the timescales for autodetachment, IC, and fragmentation.

As demonstrated by Bowen and co-workers [178, 185], DB and VB anions can be easily distinguished from one another in photoelectron spectra by both their energetics and spectral shape. DB anions are weakly bound (typically <100 meV eBE), with the excess electron residing in a large, diffuse orbital outside of the molecular framework [167]. Due to this diffuse nature, the neutral core of a DB state undergoes little or no geometry change upon photodetachment [127], yielding a narrow peak in the anion photoelectron spectrum. VB nucleobase anions typically have VDEs of hundreds of meV [166, 179, 186–189], and the geometry of VB nucleobase anions is typically distorted relative to the neutral nucleobase in the ring puckering coordinate [156, 158, 180, 181, 190], yielding a broad photoelectron spectrum [191]. Photoelectron spectra from Bowen [191], shown in Fig. 11.2 for the U^- DB anion and the

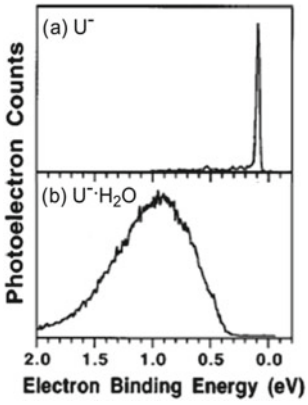

Fig. 11.2 Photoelectron spectra of **a** the U^- DB anion and **b** the $U^-{\cdot}H_2O$ VB anion. The U^- DB anion exhibits a very narrow peak at very low binding energy, characteristic of DB anions, while the $U^-{\cdot}H_2O$ VB anion exhibits a broad feature covering higher eBEs. Adapted from Ref. [191] with the permission of AIP Publishing

$U^-{\cdot}H_2O$ VB anion, exemplify the binding energy and spectral shape of these two types of negative ions.

In studies of electron attachment dynamics to nucleobases and related species, the nucleobase of interest, N, is clustered with iodide. A UV pump pulse of energy $h\nu_{pump}$ can be absorbed by the $I^-{\cdot}N$ complex to initiate charge transfer from the iodide to the nucleobase moiety, thereby creating a TNI:

$$I^-{\cdot}N \xrightarrow{h\nu_{pump}} [I\cdots N]^{*-} \tag{11.3}$$

This excitation can be carried out near the VDE of the $I^-{\cdot}N$ complex. Excitations of this nature are clearly interesting as a model for reductive DNA damage by low-energy secondary electron attachment. These complexes also exhibit a second regime of UV photoabsorption near 4.8 eV [192], which is calculated [155, 192] to encompass a strong base-centered π-π* excitation on the nucleobase with the excess electron still remaining with iodide, i.e.,

$$I^-(5p^6)\cdot N(\pi^4\pi^{*0}) \xrightarrow{h\nu_{pump}} I^-(5p^6)\cdot N(\pi^3\pi^{*1}) \tag{11.4}$$

Excitation in this UV range is also of interest in the DNA damage mechanism as the rapid, non-radiative photodeactivation pathways of π-π* UV photoexcited nucleobases are the core of the remarkable photostability of DNA [193–195]. We believe this π-π* excitation is followed by rapid charge transfer from the iodide moiety to fill the hole in the π orbital of the base to create a VB anion, as discussed in more detail in Sect. 11.5.2 and elsewhere [57].

Photoexcited $I^-{\cdot}N$ clusters can decay by a number of pathways listed in Eq. 11.5, including autodetachment, iodine loss, I^- formation, or a chemical reaction to form HI and a deprotonated nucleobase anion $[N–H]^-$.

$$\begin{aligned} I^-{\cdot}N \xrightarrow{h\nu_{pump}} [I\cdots N]^{*-} &\rightarrow I{\cdot}N + e^- \\ &\rightarrow I + N^- \rightarrow I + N + e^- \\ &\rightarrow I^- + N \\ &\rightarrow HI + [N{-}H]^- \end{aligned} \tag{11.5}$$

The $I^-{\cdot}N$ TRPES studies here have employed both the 1.58 eV Ti:Sapphire fundamental and higher energy UV probe pulses to photodetach the nascent TNIs and the possible photofragments these complexes can form, including iodide (eBE = 3.059 eV) [196], as described in more detail in the following sections.

11.4 Methodologies for I^-·Nucleobase Clusters

Figure 11.3 shows the anion TRPES experimental apparatus used by the Neumark group, which has been described in more detail previously [81, 102]. I^-·N clusters are generated by flowing 375–450 kPa of neon or argon buffer gas over a reservoir of methyl iodide. This gas mixture passes into a pulsed Even–Lavie valve operating at 500 Hz that contains a cartridge with a solid sample of the nucleobase of interest heated to 205 °C. For the I^-·CH_3NO_2 studies, the cartridge is left empty, and instead an additional reservoir on the gas line is filled with liquid CH_3NO_2 and chilled in an ice water bath. In each configuration, the gas mixture is then supersonically expanded into vacuum through a ring filament ionizer to produce cluster anions. The anions are perpendicularly extracted into a Wiley-McLaren time-of-flight mass spectrometer [197] and mass-selected to isolate the I^-·N species of interest. These ions are photodetached through their interaction with fs pump and probe laser pulses as described below. A velocity map imaging [198] spectrometer focuses the resultant photoelectrons onto a chevron-stacked position-sensitive microchannel plate detector coupled to a phosphor screen which is imaged using a charge-coupled device camera. The 3D eKE distributions are reconstructed using basis-set expansion (BASEX) methods [199].

Various pump–probe laser schemes are employed among the studies in this work. A KMLabs Griffin oscillator and Dragon amplifier are used to generate 1 kHz, 40 fs pulses centered near 790 nm (1.57 eV) with 1.8 mJ/pulse. The output of the KMLabs system is split into a pump arm and a probe arm delayed by a delay stage. In the pump arm, 1 mJ/pulse of the 1.57 eV light is used to pump a LightCon TOPAS-C optical parametric amplifier. UV light is generated by frequency doubling the TOPAS-C output with a β-barium borate (BBO) crystal to yield pump pulses between 235 and 350 nm of approximately 8–13 μJ/pulse. Pump pulses near 266 nm (~5–12 μJ/pulse) can also be generated by frequency tripling the 1.57 eV fundamental infrared (IR) of

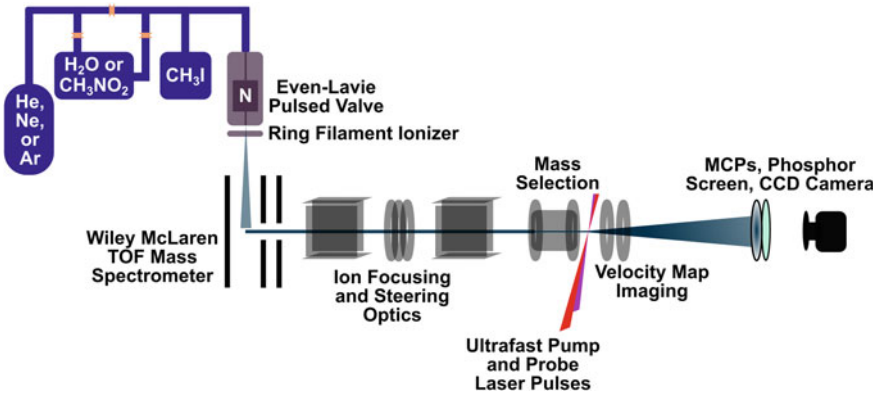

Fig. 11.3 Diagram of the anion TRPES apparatus employed by Neumark and co-workers. Reproduced from Ref. [57] with permission from the PCCP Owner Societies

the KMLabs system. The fundamental can also be used as the probe beam (1.57 eV, 80 μJ/pulse), or frequency doubled in a BBO crystal to yield 395 nm pulses (3.14 eV, 65 μJ/pulse). The residual visible non-frequency-doubled TOPAS-C output can also be recovered and recombined nonlinearly in a BBO crystal with the fundamental pulse to yield a UV probe pulse of 344 nm (8 μJ/pulse). Cross-correlations measured outside the vacuum chamber for the pump and probe laser pulses are <150 fs for UV/IR-type pump/probe schemes and ~150–200 fs for UV/UV-type pump/probe schemes.

11.5 $I^-{\cdot}CH_3NO_2$, $I^-{\cdot}U$, and $I^-{\cdot}T$ Clusters

Figure 11.4 presents the calculated structures [200] for ground state $I^-{\cdot}CH_3NO_2$, $I^-{\cdot}U$, and $I^-{\cdot}T$ at the MP2/aug-cc-pVDZ(-pp) level of theory. Table 11.1 presents the calculated dipole moments of the neutral I·N species at the equilibrium geometry of the anion, as well as the experimentally measured VDEs of the $I^-{\cdot}N$ species. To facilitate comparison between the three different systems studied here, one-photon and TRPE spectra for each species are shown in Figs. 11.5, 11.6, 11.7, and 11.8. Figure 11.5a–c shows one-photon photoelectron spectra for $I^-{\cdot}CH_3NO_2$, $I^-{\cdot}U$, and $I^-{\cdot}T$, respectively. Figure 11.6a–c shows near-VDE photoexcited TRPE spectra for each of these systems along with the time-evolution of TNI production and decay at both early and long delay times. Figure 11.7a–c shows the time-evolution of I^- production via photodissociation for $I^-{\cdot}CH_3NO_2$ and $I^-{\cdot}U$, and Fig. 11.8a, b shows

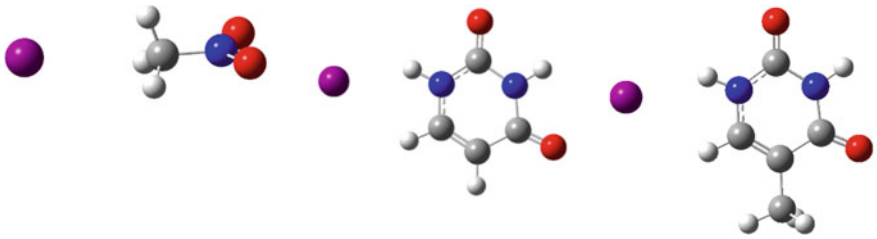

Fig. 11.4 Calculated structures for $I^-{\cdot}CH_3NO_2$ (left), $I^-{\cdot}U$ (center), and $I^-{\cdot}T$ (right). See Ref. [46] for computational details of $I^-{\cdot}CH_3NO_2$, and Ref. [156] for computational details of $I^-{\cdot}U$ and $I^-{\cdot}T$

Table 11.1 Neutral dipole moments (μ) and VDEs for the $I^-{\cdot}N$ cluster systems examined in this work. Neutral dipole moment is calculated at the ground state anion geometry. Reported VDEs are experimentally measured by single-photon anion PES, all ±0.05 eV error. See Ref. [156] for computational details of $I^-{\cdot}U$ and $I^-{\cdot}T$

Cluster	$I^-{\cdot}CH_3NO_2$	$I^-{\cdot}U$	$I^-{\cdot}T$
VDE (eV)	3.60	4.11	4.05
Neutral μ (D)	4.62	6.48	6.23

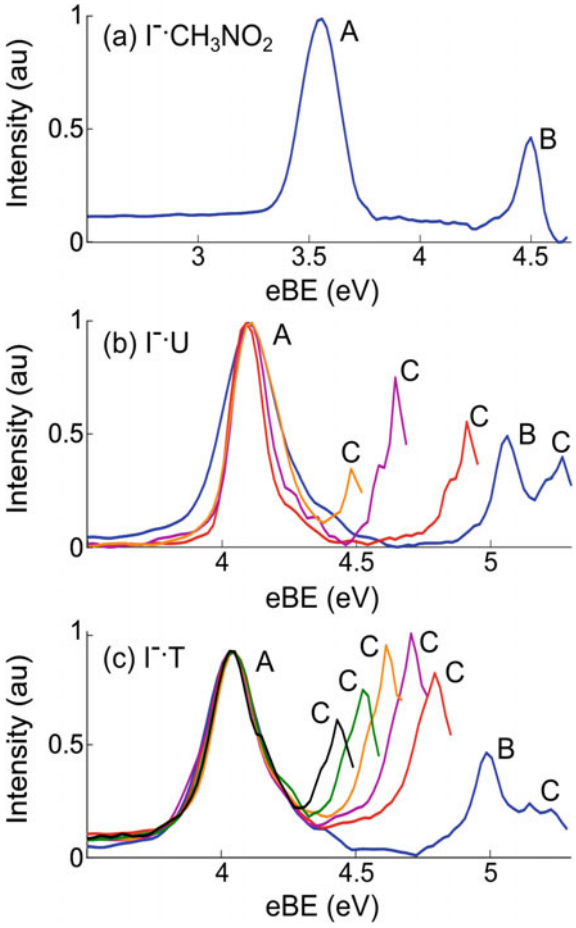

Fig. 11.5 Single-photon PE spectra for **a** $I^-{\cdot}CH_3NO_2$ with 4.68 eV; **b** $I^-{\cdot}U$ with 5.30 eV in blue, 4.92 eV in red, 4.68 eV in purple, and 4.51 eV in orange; and **c** $I^-{\cdot}T$ with 5.30 eV in blue, 4.87 eV in red, 4.78 eV in purple, 4.68 eV in orange, 4.59 eV in green, and 4.51 eV in black. "A" denotes vertical detachment to the lower spin–orbit state of the iodine-containing complex ($I(^2P_{3/2})\cdot N$), "B" denotes detachment to the upper spin–orbit state ($I(^2P_{1/2})\cdot N$), and "C" denotes autodetachment. Adapted from Ref. [57] with permission from the PCCP Owner Societies

the TRPE spectra and time-dependent signal evolution for $I^-{\cdot}U$ and $I^-{\cdot}T$ photoexcited at excitation energies near ~4.7 eV. These results are considered in more detail in the subsections below. For consistency and ease of comparison throughout this work, TRPES pump energies are given as $h\nu_{pump}$ – VDE, i.e., they are referenced to the VDE of the cluster.

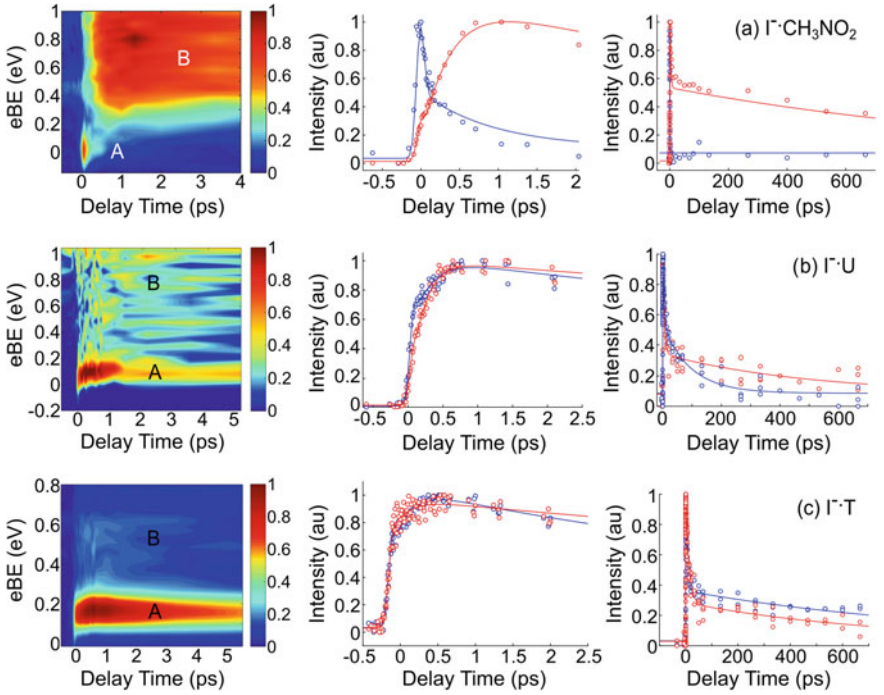

Fig. 11.6 TRPE spectra (left) and integrated intensities at both early times and long delay times (right) for the DB anion (feature A, blue) and VB anion (feature B, red) for **a** $I^-{\cdot}CH_3NO_2$ photoexcited at +0 meV; **b** $I^-{\cdot}U$ photoexcited at +30 meV; and **c** $I^-{\cdot}T$ photoexcited at +20 meV. Adapted from Ref. [57] with permission from the PCCP Owner Societies

11.5.1 $I^-{\cdot}CH_3NO_2$

We first apply TRPES to the dynamics of the photoexcited $I^-{\cdot}CH_3NO_2$ binary complex, which serves as an interesting model system for conversion between DB and VB anions and helps inform studies of the more complex uracil and thymine systems. Nitromethane (CH_3NO_2, $\mu = 3.46$ D) supports both a DB anion and a VB anion; the VB anion lies lower in energy and is the ground state of the anion [185, 201, 202]. Both DB and VB anions of $CH_3NO_2^-$ have been previously measured by single-photon PES; the DB anion has a VDE of 8 ± 8 meV, and the VB anion has a VDE of 0.9–1 eV [185, 203].

Photofragment action spectroscopy has been used by Dessent et al. to probe $I^-{\cdot}CH_3NO_2$ binary complexes, which measured the $I^-{\cdot}CH_3NO_2$ cluster VDE as 3.60 ± 0.01 eV and detected evidence for the presence of the $I^-{\cdot}CH_3NO_2$ DB anion [201]. Our group has performed two sets of TRPES studies of near-VDE photoexcited $I^-{\cdot}CH_3NO_2$ clusters at two probe energies: 1.56 eV probe experiments to examine the presence and time-resolved dynamics of DB and VB anions of nitromethane [46], and 3.14 eV probe experiments to measure the time-resolved formation of I^- and other photofragments [159].

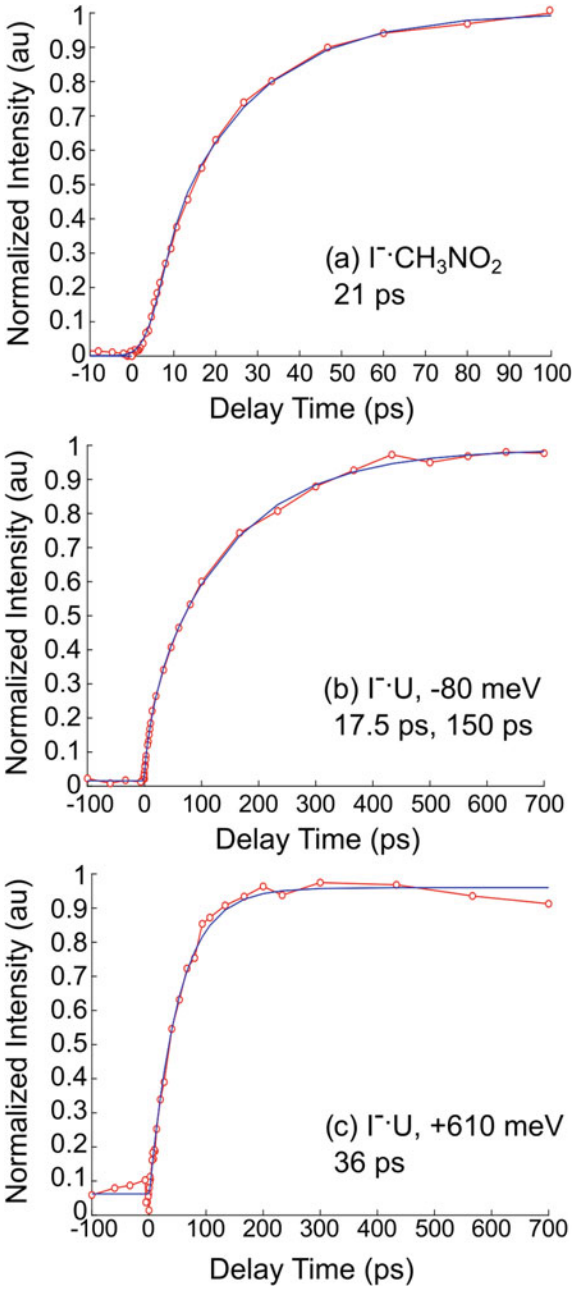

Fig. 11.7 Iodide integrated intensities for **a** $I^{-}{\cdot}CH_3NO_2$, **b** $I^{-}{\cdot}U$ photoexcited –80 meV below the VDE, and **c** $I^{-}{\cdot}U$ photoexcited at +610 meV (4.72 eV). Adapted from Ref. [57] with permission from the PCCP Owner Societies

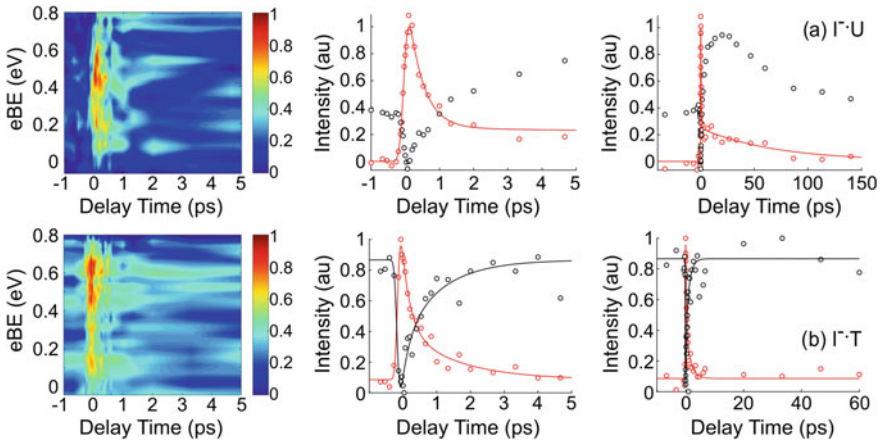

Fig. 11.8 TRPE spectra (left) and integrated intensities at both early times and long delay times (right) for the VB anion (red) and autodetachment (black) features for **a** $I^-\cdot U$ photoexcited at 4.69 eV; **b** $I^-\cdot T$ photoexcited at 4.69 eV. Reproduced from Ref. [57] with permission from the PCCP Owner Societies

Figure 11.5a shows the single-photon photoelectron spectrum of $I^-\cdot CH_3NO_2$. Feature A, centered at 3.60 eV, corresponds to the cluster VDE and matches previous experimental results for $I^-\cdot CH_3NO_2$ [201]. This feature corresponds to detachment to the lower spin–orbit state of the complex $I(^2P_{3/2})\cdot CH_3NO_2$, while feature B, appearing near 4.5 eV, corresponds to photodetachment to the upper spin–orbit state of the complex $I(^2P_{1/2})\cdot CH_3NO_2$, lying approximately 0.94 eV higher in energy [204].

TRPE spectra for $I^-\cdot CH_3NO_2$ photoexcited at 3.60 eV (at the cluster VDE) and probed at 1.56 eV are shown in Fig. 11.6a. The left panel shows a false-color contour plot of eBE as a function of pump–probe delay. Feature A is a narrow, short-lived, low eBE feature that is assigned to a DB state, while feature B is broader and longer lived, assigned to a VB state. The center and right panels of Fig. 11.6a present integrated intensities of feature A (blue) and feature B (red) at short and longer time delays, respectively. A similar layout is used for the other rows of Fig. 11.6. The nascent $[I\cdots CH_3NO_2]^-$ DB anion appears within the cross-correlation of the pump and probe laser pulses, <150 fs, and decays mono-exponentially in 460 ± 60 fs, while the $[I\cdots CH_3NO_2]^-$ VB anion appears in 420 ± 50 fs [46]. These congruent lifetimes indicate that the DB anion decays primarily to form the VB anion in a rapid and complete or nearly complete conversion. The VB state was found to decay bi-exponentially with time constants of 2 and 1300 ps.

A second TRPES study with 3.56 eV pump energy (–40 meV) and 3.14 eV probe energy was performed to characterize the decay dynamics of the $[I\cdots CH_3NO_2]^-$ VB anion [159]. This probe energy is high enough to detect photodissociation products such as I^- (eBE = 3.059 eV) [196] and the nitromethide anion $CH_2NO_2^-$ (VDE = 2.635 ± 0.010 eV) [159, 205]. I^- is measured as the major photofragmentation channel with a mono-exponential rise time of 21 ± 1 ps, which is shown in

Fig. 11.7a. This finding suggests that the 2 ps VB anion decay lifetime corresponds to back-electron transfer to reform $I^-{\cdot}CH_3NO_2$, followed by IC to the $I^-{\cdot}CH_3NO_2$ anion ground state and, finally, dissociation to yield I^- in 21 ps.

Rice–Ramsperger–Kassel–Marcus (RRKM) calculations were performed to analyze the statistical unimolecular dissociation of $I^-{\cdot}CH_3NO_2$ complexes to determine if the 21 ps I^- formation from 2 ps VB anion decay is a statistical process [159, 206, 207]. These RRKM calculations yield dissociation rates of only 300–400 fs, and this rapid lifetime is unlikely to be a realistic physical timescale for intramolecular vibrational energy redistribution (IVR) and subsequent dissociation in a cluster. This result indicates that there exists a dynamical bottleneck in the formation of I^- from $I^-{\cdot}CH_3NO_2$.

We have suggested that such a bottleneck arises in $I^-{\cdot}CH_3NO_2$ from inefficient energy flow from high-frequency $–NO_2$ vibrational modes in the VB anion to the relatively low-frequency (<100 cm^{-1}) $I{\cdots}CH_3NO_2$ modes that ultimately yield I^- dissociation [159]. The $[I{\cdots}CH_3NO_2]^-$ DB anion should geometrically resemble neutral $I{\cdot}CH_3NO_2$, while the $[I{\cdots}CH_3NO_2]^-$ VB anion is expected to more closely resemble the puckered $CH_3NO_2{}^-$ geometry in which the $–NO_2$ is out of the plane of the molecule [46, 203]. Hence, during the DB to VB anion transition, the $–NO_2$ vibrational modes become vibrationally excited. Previous theoretical work of gas-phase S_N2-type reactions has shown that energy transfer between high-energy and low-energy vibrational modes in a binary complex may be inefficient and lead to non-statistical dynamics [208–212] Thus, IVR within the reformed $I^-{\cdot}CH_3NO_2$ complex can act as the rate-limiting step in cluster dissociation and cause the delayed I^- rise observed here.

Autodetachment from photoexcited $I^-{\cdot}CH_3NO_2$ clusters was also measured as near ~0 eV eKE photoelectron signal [46]. Autodetachment, the spontaneous ejection of an electron following photoexcitation of an anion resonance, can occur if the resonance lies isoenergetically within a manifold of vibrational levels of the corresponding neutral plus a free electron. The ejection is thus facilitated by nonadiabatic coupling between the electronic and nuclear degrees of freedom in the system [127, 213, 214]. If the internal energy of the excited anion (or cluster) is randomized prior to electron ejection, the detached electron typically carries ~0 eV eKE and this statistical process is referred to as thermionic emission [215, 216]. We expect, then, that the long 1300 ps VB anion decay corresponds to autodetachment.

To summarize these photoexcited $I^-{\cdot}CH_3NO_2$ decay dynamics, we conclude that the 2 ps decay of the VB anion is IC to the ground state followed by delayed I^- evaporation, and the long, 1300 ps VB anion decay is by autodetachment, as in Eq. 11.6:

$$\begin{aligned} I^-{\cdot}CH_3NO_2 &\xrightarrow{h\nu_{\text{pump}}} [I\cdots CH_3NO_2]^{*-}_{DB} \rightarrow [I\cdots CH_3NO_2]^{*-}_{VB} \\ [I\cdots CH_3NO_2]^{*-}_{VB} &\xrightarrow[\text{Conversion}]{\text{Internal}} I^-{\cdot}CH_3NO_2 \xrightarrow[\text{Dissociation}]{\text{Delayed}} I^- + CH_3NO_2 \\ &\xrightarrow{\text{Autodetachment}} I{\cdot}CH_3NO_2 + e^- \end{aligned} \tag{11.6}$$

These measured dynamics for near-VDE photoexcited $I^-{\cdot}CH_3NO_2$ complexes provide insight into the dynamics and energetics of the TNIs and also the possible interactions between the iodine atom and the CH_3NO_2 moiety. We consider these results in the discussion of the $I^-{\cdot}U$ and $I^-{\cdot}T$ studies in the following sections.

11.5.2 I^-·Uracil and I^-·Thymine Binary Complexes

The pyrimidine bases uracil and thymine each have a sufficiently large dipole moment to support a DB anion ($\mu \sim 4.15$ D) [169]. Single-photon PES measured by Bowen [178] finds the uracil and thymine DB anions to have eBEs of approximately 90 meV and 70 meV, respectively. No VB anions of either base have been detected in previous PES studies, but Rydberg electron transfer experiments [187] and theoretical calculations [186, 217] predict that both the DB anion and the VB anion for both uracil and thymine exist, at least as metastable TNIs, with VB anion VDEs of approximately 500 meV. For both nucleobases, the DB anion is the anionic ground state [191, 218], with a calculated barrier of 36–155 meV for conversion to form the VB anion, depending on the level of theory used [156]. However, bare thymine is calculated to have a ~10–20 meV higher conversion barrier for DB to VB anion conversion than bare uracil at each level of theory employed.

TRPES has been used to study the time-resolved dynamics of $I^-{\cdot}U$ and $I^-{\cdot}T$ clusters at photoexcitation energies near the VDE [154, 156] as well as in the higher energy (~4.6–4.9 eV) excitation regime [152, 153, 155]. Here, we first briefly cover single-photon PES results as well as laser photodissociation spectroscopy experiments on $I^-{\cdot}U$ and $I^-{\cdot}T$ by the Dessent group and excited state calculations to provide context for the discussion of the time-resolved work [155, 192].

Single-photon PE spectra collected at multiple photon energies for $I^-{\cdot}U$ and $I^-{\cdot}T$ are overlaid and reproduced in Fig. 11.5b and 11.5c, respectively [152, 153]. Feature A corresponds to direct detachment to the $I(^2P_{3/2}){\cdot}N$ neutral complex, yielding a VDE of 4.11 ± 0.05 eV for $I^-{\cdot}U$ and 4.05 eV ± 0.05 eV for $I^-{\cdot}T$. Feature B, seen only at the highest photon energies, arises from photodetachment to the upper iodine spin–orbit state. Feature C is present at each detachment energy at ~0 eV eKE and corresponds to autodetachment. Interestingly, we note that the intensity of the autodetachment signal appears to reach a maximum near 4.7–4.8 eV photon energy, and declines at energies above and below this region.

Laser photodissociation spectroscopy has been carried out on $I^-{\cdot}U$ and $I^-{\cdot}T$ by Dessent et al. [155, 192] for $I^-{\cdot}U$ and $I^-{\cdot}T$ clusters to measure their photoabsorption profiles as well as photofragment formation as a function of pump energy. Figure 11.9a and 11.9b shows the photodepletion (photoabsorption, including dissociation and detachment) profiles for $I^-{\cdot}U$ and $I^-{\cdot}T$, respectively, from 3.6 to 5.3 eV. Two regimes of UV photoabsorption are measured: the first excited state near the VDE, approximately 4 eV for both clusters, and the second centered around 4.8 eV. The photofragmentation results find I^- and $[N–H]^-$, the deprotonated nucleobase anion, as photofragments for both clusters, with I^- appearing as the overwhelmingly

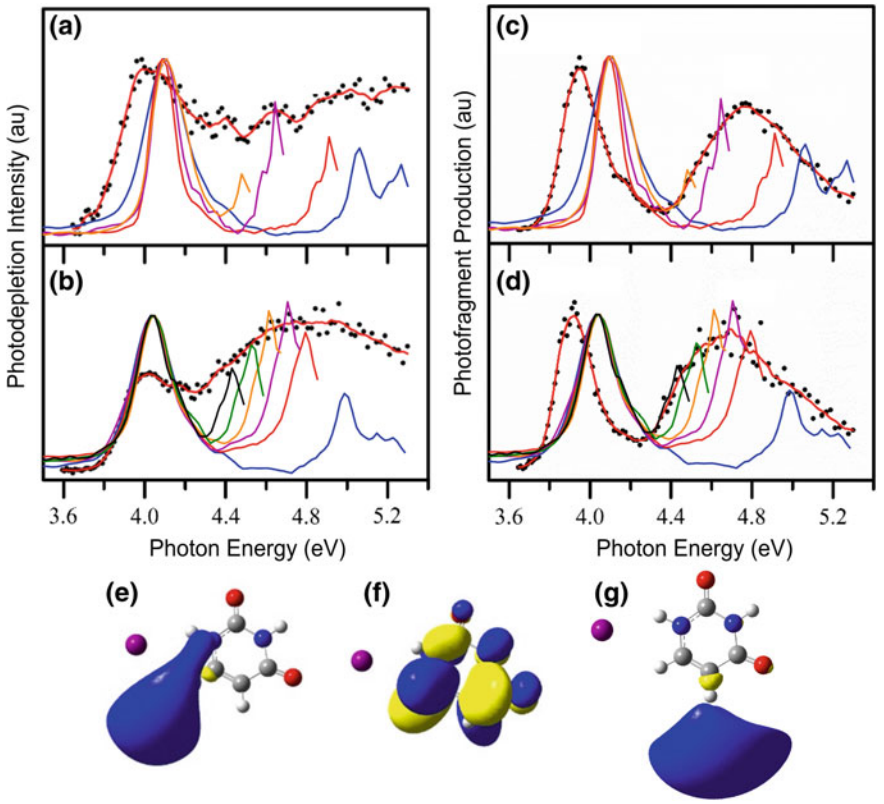

Fig. 11.9 Overlay of the single-photon PE spectra from Fig. 11.5b for $I^-\cdot U$ and Fig. 11.5c for $I^-\cdot T$ with the laser photodissociation spectroscopy results from Ref. [192]. **a** Photodepletion (absorption) for $I^-\cdot U$ clusters photoexcited between 3.6 and 5.3 eV and **b** for $I^-\cdot T$ clusters. **c** I^- formation from photoexcited $I^-\cdot U$ clusters and **d** I^- formation from photoexcited $I^-\cdot T$ clusters. Photoelectron spectra are normalized to match the photodissociation data (black dots). **e** EOM-CCSD/aug-cc-pVDZ(-pp) calculated image of the $I^-\cdot U$ DB orbital and **f** for the π^* orbital and **g** for the σ^* orbital for transitions localized near 4.7 eV. Reproduced from Ref. [57] with permission from the PCCP Owner Societies

dominant species [192]. Figure 11.9c and 11.9d presents the photofragment yields of I^- for $I^-\cdot U$ and $I^-\cdot T$, respectively. Both photofragments are also found in two distinct bands of photoexcitation: one centered near the VDE of each cluster and one centered near 4.8 eV.

In Fig. 11.9, we also overlay these laser photodissociation results with the respective $I^-\cdot U$ and $I^-\cdot T$ one color photoelectron spectra from Fig. 11.5b, c. The VDE photodetachment features appear at energies slightly above the first photoabsorption and photofragmentation bands; this occurs because photodetachment is not possible below the VDE, but photoabsorption and formation of the DB anion is possible and has been measured at pump energies below the VDE, as described in more detail below [154–156, 192]. Note that the single-photon PES autodetachment feature for

both I^-·U and I^-·T appears to track closely with the higher energy photoabsorption and I^- photofragmentation bands; we discuss this and the dynamics resulting from high-energy photoexcitation in more detail in Sect. 11.5.2.3.

To examine the nature of the photoexcitation in each of the two measured energy regimes, excited state calculations have been performed at the TD-DFT/B3LYP level for I^-·U and I^-·T [192], and at the EOM-CCSD/aug-cc-pVDZ(-pp) level for I^-·U [155]. Near the I^-·U VDE, the EOM-CCSD calculation finds three optical transitions with prominent oscillator strength corresponding to excitation from an iodide (5*p*) orbital to form a DB state of the complex (Fig. 11.9e). Both sets of excited state calculations find by far the strongest transition near 4.8 eV to be a base-centered π-π* excitation (Fig. 11.9f). Much weaker transitions near 4.7 eV, corresponding to excitation from an iodide (5*p*) orbital to a σ* state of the complex (Fig. 11.9g), are also found; the oscillator strength is lower by a factor ranging from two to 18 depending on the cluster and the method. No evidence is found for channels with significant oscillator strength corresponding to I(5*p*) → π* charge transfer, i.e., direct optical excitation to form the VB anion, presumably reflecting near-zero spatial overlap between these initial and final states. Thus, we expect that near-VDE photoexcitation likely yields direct optical excitation from iodide to form the DB anion instantaneously, while photoexcitation at higher pump energies will likely yield dynamics with the largest contribution from base-centered π-π* excitation. We now turn our attention to the time-resolved results of photoexcited I^-·U and I^-·T clusters in each of these two pump energy regimes.

11.5.2.1 Early Time Dynamics from Near-VDE Excitation of I^-·U and I^-·T

TRPES studies of I^-·U and I^-·T clusters were carried out at pump excitation energies from ~±100 meV relative to the VDE [154, 156], and are shown in Fig. 11.6b and 11.6c for I^-·U at +30 meV and I^-·T at +20 meV, respectively. At each of these excitation energies, both the DB anion (feature A, blue) and the VB anion (feature B, red) of each cluster are observed. In I^-·U, the DB anion rise time decreases from approximately 250 fs to ≤150 fs as the pump energy is increased, while the VB anion rise time remains near 250 fs over this pump energy range. In I^-·T, the DB anion appears in approximately 230 fs, exhibiting no dependence on the pump excitation energy, and the VB anion forms in approximately 300 fs.

These results indicate that while the DB state is formed first and followed in appearance by the VB anion, because the DB signal remains while the VB signal grows in, both I^-·U and I^-·T seem to exhibit at most only partial DB to VB anion conversion. The excited state calculations in Sect. 11.5.2 show that there is direct optical excitation to form a DB state but no optical transition to form the VB state, indicating that the origin of the VB signal is expected to be from DB to VB anion conversion. Given that the DB anion is the anionic ground state for uracil and thymine [191, 218] and there is expected to be an uphill barrier of ~36–55 meV for conversion [156], it is reasonable that only partial DB to VB anion conversion occurs, in

comparison, for example, to the rapid and complete DB to VB anion conversion in $I^-{\cdot}CH_3NO_2$.

11.5.2.2 Long Time Dynamics of Near-VDE Excited $I^-{\cdot}U$ and $I^-{\cdot}T$ Clusters

The DB and VB anions of near-VDE photoexcited $I^-{\cdot}U$ and $I^-{\cdot}T$ clusters decay bi-exponentially, with each set of lifetimes generally decreasing with increasing pump excitation energy. For $I^-{\cdot}U$ photoexcited at +30 meV (Fig. 11.6b), the DB anion decay constants are 5.0 and 500 ps, while the VB anion decays in 5.6 and 80 ps [154]. $I^-{\cdot}T$ photoexcited at +20 meV (Fig. 11.6c) similarly exhibits DB anion decay in 5.2 and 1100 ps, and VB anion decay in 13.1 and 530 ps [156].

TRPES of near-VDE photoexcited $I^-{\cdot}U$ clusters finds two decay pathways: autodetachment and bi-exponential reformation of I^- [154, 155]. TRPES of $I^-{\cdot}U$ clusters photoexcited at 4.03 eV (−80 meV) and probed at 3.61 eV measures bi-exponential formation of I^- in 17.5 ± 1.6 ps and 150 ± 10 ps as the only major photodissociation pathway; this I^- rise signal is shown in Fig. 11.7b. These bi-exponential I^- rise dynamics can be assigned in light of the mechanism of I^- reformation in $I^-{\cdot}CH_3NO_2$ (Eq. 11.6). For $I^-{\cdot}U$ clusters, since both TNIs are present as the DB to VB anion conversion is only partially complete, we expect that each TNI has a fast decay process of IC to the electronic $I^-{\cdot}U$ ground state followed by evaporation of I^- to ultimately yield bi-exponential I^- rise. We attribute the fast I^- appearance to IC of the DB anion, and the slow I^- appearance of 150 ps to IC and delayed ejection of I^- from the VB anion, as the VB anion decay may also have a dynamical bottleneck similar to that observed in $I^-{\cdot}CH_3NO_2$. The overall decay mechanisms for the DB and VB anions are summarized in Eq. 11.7.

$$
\begin{aligned}
I^-{\cdot}N &\xrightarrow{h\nu_{\text{pump}}} [I\cdots N]^{*-}_{DB}, [I\cdots N]^{*-}_{VB} \\
[I\cdots N]^{*-}_{DB} &\xrightarrow[\text{Conversion}]{\text{Internal}} I^-{\cdot}N \rightarrow I^- + N \\
&\xrightarrow{\text{Autodetachment}} I{\cdot}N + e^- \\
[I\cdots N]^{*-}_{VB} &\xrightarrow[\text{Conversion}]{\text{Internal}} I^-{\cdot}N \xrightarrow[\text{Dissociation}]{\text{Delayed}} I^- + N \\
&\xrightarrow{\text{Autodetachment}} I{\cdot}N + e^-
\end{aligned}
\tag{11.7}
$$

The long time decays of each TNI for both species are likely by autodetachment, or rather, more specifically, by thermionic emission considering the ~100 ps–1 ns long decay lifetimes and measured decrease in the long time constants with increasing pump energy. Laser photodissociation spectra found $[U–H]^-$ (neutral electron affinity = 3.481 eV) [219] as an additional minor dissociation product from $I^-{\cdot}U$ clusters; this channel was not measured by TRPES, most likely due to its low abundance and broad photoelectron spectral profile [155, 220].

11.5.2.3 Dynamics of I^-·U and I^-·T Excited at Higher Energy

TRPE spectra of I^-·U and I^-·T photoexcited at 4.69 eV and probed at 1.57 eV are shown in Fig. 11.8a and 11.8b, respectively [152, 153]. No evidence for the existence of a DB state is measured for either cluster in this pump energy regime, but both species exhibit VB anion signal (red integrated intensity) with a cross-correlation limited rise (≤150 fs), as well as ~0 eV eKE signal corresponding to autodetachment (black integrated intensity). The I^-·U VB anion decays bi-exponentially in 620 fs and 52 ps, while the I^-·T VB anion undergoes mono-exponential decay [156] in ~610 fs. The autodetachment signal for both clusters exhibits nonzero autodetachment intensity at negative times (i.e., pump only), prompt depletion at t = 0 fs, and recovery to the initial intensity, although in I^-·U clusters the signal is found to exceed its initial intensity. The I^-·T VB anion prompt appearance and decay dynamics mirror that of the autodetachment signal, as seen in the integrated intensities in Fig. 11.8b [153].

Experiments on I^-·U at pump and probe energies of 4.72 eV and 3.15 eV, respectively, find formation of I^- to be the dominant photodissociation channel; mono-exponential appearance of I^- occurs in 36 ± 3 ps (Fig. 11.7c). An analogous high-energy probe study has not yet been performed for I^-·T clusters, but the laser photodissociation spectroscopy results confirm that I^- is the major photofragment produced from both sets of photoexcited clusters [192]. It is apparent in Fig. 11.8 that, for both I^-·U and I^-·T clusters, the VB anion appearance and fast decay dynamics match closely with the autodetachment depletion and recovery. It is also striking from the overlay of the single-photon PE spectra with the I^- photofragment formation results in Fig. 11.9c, d that the autodetachment signal tracks closely with the I^- photofragment production. Thus, it appears that I^- formation, autodetachment, and the VB anion share one common dynamical origin that is similar in nature for both clusters.

Given that one dynamical process is expected to give rise to all three of these features and that the excited state calculations for both I^-·U and I^-·T clusters find very strong oscillator strength for a base-centered π-π* excitation in this energy regime, it is likely that the pump pulse creates a π-π* excited state that is responsible for the observed dynamics [57]. Two possible channels following π-π* excitation are IC to the I^-·N ground state to yield cluster dissociation to produce I^-, as in Eq. 11.8, and charge transfer from iodide to the base moiety to fill the hole in the π orbital, essentially creating a VB anion that may then undergo autodetachment (Eq. 11.9).

$$I^- \cdot N \xrightarrow{h\nu_{\text{pump}}} I^- \cdot N(\pi^3\pi^{*1}) \xrightarrow[\text{Conversion}]{\text{Internal}} I^- \cdot N \rightarrow I^- + N \tag{11.8}$$

$$\rightarrow I \cdot N(\pi^4\pi^{*1}) \xrightarrow{\text{Autodetachment}} I \cdot N + e^- \tag{11.9}$$

We have thus previously proposed that in both I^-·U and I^-·T, photoexcitation from ~4.6 to 4.8 eV creates a π-π* excited state, some fraction of which may decay

by IC to the $I^-\cdot N$ ground state followed by dissociation to produce I^- (Eq. 11.8), and another fraction of which may have charge transfer within the cross-correlation of the pump and probe laser pulses from the iodide moiety to produce a VB anion that then decays by autodetachment (Eq. 11.9) [57]. These proposed pathways are summarized for the approximate energies and ranges of the excited states of $I^-\cdot U$ in Fig. 11.10. This figure also shows the $I^-\cdot U$ near-VDE photoexcitation dynamics as described in the earlier subsections of Sect. 11.5.2.

Some portions of this π-π^* photoexcitation mechanism are not fully explained and would benefit considerably from a more extensive theoretical investigation into the nature and energetics of the photoexcited states accessible in this pump energy region. For example, it is challenging to explain the rapid rate of charge transfer from iodide to the π orbital and instantaneous VB anion formation given the lack of overlap between these two orbitals. Additionally, $I^-\cdot U$ exhibits long-lived dynamics that are not present in $I^-\cdot T$, and it is unclear why the $I^-\cdot U$ VB anion exhibits both fast and slow decay by autodetachment, although we have put forth such mechanistic explanations previously [152–154, 156].

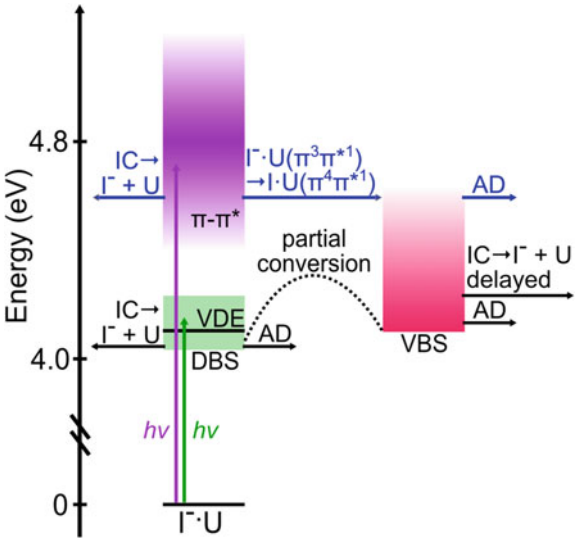

Fig. 11.10 Diagram of the proposed $I^-\cdot U$ dynamical pathways resulting from near-VDE photoexcitation (green photon, black arrows) and higher energy photoexcitation (purple photon, blue arrows). DBS and VBS denote the DB and VB states, respectively. Reproduced from Ref. [57] with permission from the PCCP Owner Societies

11.6 Summary and Outlook

The application of TRPES to molecular anions and clusters has proven to be an opportune method to explore the nature of fundamental ultrafast interactions of solvents and molecules with excess electrons. This versatile technique has been applied to a number of different solvent systems, multiply charged species, and biomolecular anions to uncover relaxation mechanisms and ultrafast charge accommodation dynamics. Specifically, TRPES of $I^-{\cdot}N$ clusters has revealed the ultrafast formation and conversion of nucleobase TNIs thought to be important in reductive damage pathways in DNA.

There are many promising future directions for work of this kind, including microhydration of $I^-{\cdot}N$ clusters, specifically $I^-{\cdot}U{\cdot}H_2O$ complexes [157]. The stepwise addition of individual water molecules building up to a solvation shell will allow for comparison between gas-phase dynamics of nucleobases and those recorded in bulk solution. In this regard, TRPES experiments in our group [221] and elsewhere [222, 223] on the dynamics of nucleic acid constituents in liquid water microjets are of particular interest. The future implementation of a new cluster source to our apparatus, such as one based on electrospray ionization [15], will enable TRPES studies of larger biomolecules such as nucleosides and nucleotides, with the ultimate goal of inducing electron attachment and monitoring not only the initial site of electron attachment and the TNI dynamics but also probing photofragment formation to measure the identities and timescales for formation of photodissociation products in these larger nucleic acid constituents.

Acknowledgements This research was funded by the National Science Foundation under Grant No. CHE-1663832. A.K. acknowledges Government support awarded by DoD, Air Force Office of Scientific Research, National Defense Science and Engineering Graduate (NDSEG) Fellowship, 32 CFR 168a. D.M.N. thanks the many graduate students and postdoctoral fellows who carried out the work in his laboratory that is reported here.

References

1. Yang, S.H., Pettiette, C.L., Conceicao, J., Cheshnovsky, O., Smalley, R.E.: Chem. Phys. Lett. **139**, 233 (1987)
2. Yang, S., Taylor, K.J., Craycraft, M.J., Conceicao, J., Pettiette, C.L., Cheshnovsky, O., Smalley, R.E.: Chem. Phys. Lett. **144**, 431 (1988)
3. Ganteför, G., Gausa, M., Meiwes-Broer, K.-H., Lutz, H.O.: Faraday Discuss. Chem. Soc. **86**, 197 (1988)
4. Ho, J., Ervin, K.M., Lineberger, W.C.: J. Chem. Phys. **93**, 6987 (1990)
5. Zubarev, D.Y., Averkiev, B.B., Zhai, H.-J., Wang, L.-S., Boldyrev, A.I.: Phys. Chem. Chem. Phys. **10**, 257 (2008)
6. Wang, L.-M., Wang, L.-S.: Nanoscale **4**, 4038 (2012)
7. Haberland, H., Bowen, K.H.: In: Haberland, H. (ed.) Clusters of Atoms and Molecules. Springer, Heidelberg (1993)
8. Robertson, W.H., Johnson, M.A.: Annu. Rev. Phys. Chem. **54**, 173 (2003)

9. Coe, J.V., Williams, S.M., Bowen, K.H.: Int. Rev. Phys. Chem. **27**, 27 (2008)
10. Sanov, A., Carl Lineberger, W.: Phys. Chem. Comm. **5**, 165 (2002)
11. Verlet, J.R.R.: Chem. Soc. Rev. **37**, 505 (2008)
12. Young, R.M., Neumark, D.M.: Chem. Rev. **112**, 5553 (2012)
13. Davis, A.V., Zanni, M.T., Frischkorn, C., Neumark, D.M.: J. Electron Spectrosc. Relat. Phenom. **108**, 203 (2000)
14. Boudaiffa, B., Cloutier, P., Hunting, D., Huels, M.A., Sanche, L.: Science **287**, 1658 (2000)
15. Anstöter, C.S., Bull, J.N., Verlet, J.R.R.: Int. Rev. Phys. Chem. **35**, 509 (2016)
16. Stolow, A., Bragg, A.E., Neumark, D.M.: Chem. Rev. **104**, 1719 (2004)
17. Fielding, H.H., Worth, G.A.: Chem. Soc. Rev. **47**, 309 (2018)
18. Suzuki, T.: Annu. Rev. Phys. Chem. **57**, 555 (2006)
19. Hayden, C.C., Stolow, A.: Photoionization and Photodetachment, p. 91. World Scientific (2000)
20. Neumark, D.M.: Annu. Rev. Phys. Chem. **52**, 255 (2001)
21. Suzuki, T., Whitaker, B.J.: Int. Rev. Phys. Chem. **20**, 313 (2001)
22. Stolow, A.: Annu. Rev. Phys. Chem. **54**, 89 (2003)
23. Stolow, A.: Int. Rev. Phys. Chem. **22**, 377 (2003)
24. Suzuki, T.: Modern Trends in Chemical Reaction Dynamics, p. 529 World Scientific (2004)
25. Wollenhaupt, M., Engel, V., Baumert, T.: Annu. Rev. Phys. Chem. **56**, 25 (2004)
26. Stolow, A., Underwood, J.G.: Adv. Chem. Phys. (2008)
27. Stavros, V.G., Verlet, J.R.R.: Annu. Rev. Phys. Chem. **67**, 211 (2016)
28. Spesyvtsev, R., Underwood, J.G., Fielding, H.H.: In: de Nalda, R., Bañares, L. (eds.) Ultrafast Phenomena in Molecular Sciences: Femtosecond Physics and Chemistry, p. 99. Springer International Publishing, Cham (2014)
29. Corderman, R.R., Lineberger, W.C.: Annu. Rev. Phys. Chem. **30**, 347 (1979)
30. Posey, L.A., Deluca, M.J., Johnson, M.A.: Chem. Phys. Lett. **131**, 170 (1986)
31. Cheshnovsky, O., Yang, S.H., Pettiette, C.L., Craycraft, M.J., Liu, Y., Smalley, R.E.: Chem. Phys. Lett. **138**, 119 (1987)
32. Arnold, S., Coe, J., Eaton, J., Freidhoff, C., Kidder, L., Lee, G., Manaa, M., McHugh, K., Patel-Misra, D., Sarkas, H., Snodgrass, J., Bowen, K.: In: Scholes, G. (ed.) The Chemical Physics of Atomic and Molecular Clusters. North-Holland Amsterdam (1990)
33. Wang, X.-B., Wang, L.-S.: Annu. Rev. Phys. Chem. **60**, 105 (2009)
34. Lineberger, W.C.: Annu. Rev. Phys. Chem. **64**, 21 (2013)
35. Wang, L.-S.: Int. Rev. Phys. Chem. **35**, 69 (2016)
36. Paik, D.H., Lee, I.R., Yang, D.-S., Baskin, J.S., Zewail, A.H.: Science **306**, 672 (2004)
37. Frischkorn, C., Bragg, A.E., Davis, A.V., Wester, R., Neumark, D.M.: J. Chem. Phys. **115**, 11185 (2001)
38. Bragg, A.E., Wester, R., Davis, A.V., Kammrath, A., Neumark, D.M.: Chem. Phys. Lett. **376**, 767 (2003)
39. Pontius, N., Bechthold, P.S., Neeb, M., Eberhardt, W.: Phys. Rev. Lett. **84**, 1132 (2000)
40. Pontius, N., Lüttgens, G., Bechthold, P.S., Neeb, M., Eberhardt, W.: J. Chem. Phys. **115**, 10479 (2001)
41. Niemietz, M., Gerhardt, P., Ganteför, G., Dok Kim, Y.: Chem. Phys. Lett. **380**, 99 (2003)
42. Pontius, N., Neeb, M., Eberhardt, W., Lüttgens, G., Bechthold, P.S.: Phys. Rev. B **67**, 035425 (2003)
43. Stanzel, J., Burmeister, F., Neeb, M., Eberhardt, W., Mitrić, R., Bürgel, C., Bonačić-Koutecký, V.: J. Chem. Phys. **127**, 164312 (2007)
44. Niemietz, M., Engelke, M., Kim, Y.D., Ganteför, G.: Phys. Rev. B **75**, 085438 (2007)
45. Griffin, G.B., Ehrler, O.T., Kammrath, A., Young, R.M., Cheshnovsky, O., Neumark, D.M.: J. Chem. Phys. **130**, 231103 (2009)
46. Yandell, M.A., King, S.B., Neumark, D.M.: J. Chem. Phys. **140**, 184317 (2014)
47. Bull, J.N., Verlet, J.R.R.: Sci. Adv. **3**, e1603106 (2017)
48. Rogers, J.P., Anstöter, C.S., Verlet, J.R.R.: Nat. Chem. **10**, 341 (2018)

49. Ehrler, O.T., Yang, J.-P., Sugiharto, A.B., Unterreiner, A.N., Kappes, M.M.: J. Chem. Phys. **127**, 184301 (2007)
50. Dau, P.D., Liu, H.-T., Yang, J.-P., Winghart, M.-O., Wolf, T.J.A., Unterreiner, A.-N., Weis, P., Miao, Y.-R., Ning, C.-G., Kappes, M.M., Wang, L.-S.: Phys. Rev. A **85**, 064503 (2012)
51. Winghart, M.-O., Yang, J.-P., Kühn, M., Unterreiner, A.-N., Wolf, T.J.A., Dau, P.D., Liu, H.-T., Huang, D.-L., Klopper, W., Wang, L.-S., Kappes, M.M.: Phys. Chem. Chem. Phys. **15**, 6726 (2013)
52. Verlet, J.R.R., Horke, D.A., Chatterley, A.S.: Phys. Chem. Chem. Phys. **16**, 15043 (2014)
53. Lee, I.R., Lee, W., Zewail, A.H.: Proc. Natl. Acad. Sci. U.S.A. **103**, 258 (2006)
54. Horke, D.A., Li, Q., Blancafort, L., Verlet, J.R.R.: Nat. Chem. **5**, 711 (2013)
55. Mooney, C.R.S., Horke, D.A., Chatterley, A.S., Simperler, A., Fielding, H.H., Verlet, J.R.R.: Chem. Sci. **4**, 921 (2013)
56. Chatterley, A.S., West, C.W., Stavros, V.G., Verlet, J.R.R.: Chem. Sci. **5**, 3963 (2014)
57. Kunin, A., Neumark, D.M.: Phys. Chem. Chem. Phys. **21**, 7239–7255 (2019)
58. Bragg, A.E., Verlet, J.R.R., Kammrath, A., Neumark, D.M.: J. Chem. Phys. **121**, 3515 (2004)
59. Ehrler, O.T., Yang, J.P., Hättig, C., Unterreiner, A.-N., Hippler, H., Kappes, M.M.: J. Chem. Phys. **125**, 074312 (2006)
60. Paik, D.H., Bernhardt, T.M., Kim, N.J., Zewail, A.H.: J. Chem. Phys. **115**, 612 (2001)
61. Paik, D.H., Kim, N.J., Zewail, A.H.: J. Chem. Phys. **118**, 6923 (2003)
62. Kim, N.J., Paik, D.H., Zewail, A.H.: J. Chem. Phys. **118**, 6930 (2003)
63. Paik, D.H., Baskin, J.S., Kim, N.J., Zewail, A.H.: J. Chem. Phys. **125**, 133408 (2006)
64. Verlet, J.R.R., Bragg, A.E., Kammrath, A., Cheshnovsky, O., Neumark, D.M.: J. Chem. Phys. **121**, 10015 (2004)
65. Bragg, A.E., Verlet, J.R.R., Kammrath, A., Cheshnovsky, O., Neumark, D.M.: J. Chem. Phys. **122**, 054314 (2005)
66. Griffin, G.B., Kammrath, A., Ehrler, O.T., Young, R.M., Cheshnovsky, O., Neumark, D.M.: Chem. Phys. **350**, 69 (2008)
67. Young, R.M., Griffin, G.B., Ehrler, O.T., Kammrath, A., Bragg, A.E., Verlet, J.R.R., Cheshnovsky, O., Neumark, D.M.: Phys. Scr. **80**, 048102 (2009)
68. Greenblatt, B.J., Zanni, M.T., Neumark, D.M.: Chem. Phys. Lett. **258**, 523 (1996)
69. Greenblatt, B.J., Zanni, M.T., Neumark, D.M.: Science **276**, 1675 (1997)
70. Greenblatt, B.J., Zanni, M.T., Neumark, D.M.: Faraday Discuss. **108**, 101 (1997)
71. Zanni, M.T., Taylor, T.R., Greenblatt, B.J., Soep, B., Neumark, D.M.: J. Chem. Phys. **107**, 7613 (1997)
72. Zanni, M.T., Greenblatt, B.J., Neumark, D.M.: J. Chem. Phys. **109**, 9648 (1998)
73. Greenblatt, B.J., Zanni, M.T., Neumark, D.M.: J. Chem. Phys. **111**, 10566 (1999)
74. Greenblatt, B.J., Zanni, M.T., Neumark, D.M.: J. Chem. Phys. **112**, 601 (1999)
75. Zanni, M.T., Batista, V.S., Greenblatt, B.J., Miller, W.H., Neumark, D.M.: J. Chem. Phys. **110**, 3748 (1999)
76. Davis, A.V., Zanni, M.T., Frischkorn, C., Elhanine, M., Neumark, D.M.: J. Electron Spectrosc. Relat. Phenom. **112**, 221 (2000)
77. Zanni, M.T., Davis, A.V., Frischkorn, C., Elhanine, M., Neumark, D.M.: J. Chem. Phys. **112**, 8847 (2000)
78. Davis, A.V., Wester, R., Bragg, A.E., Neumark, D.M.: J. Chem. Phys. **117**, 4282 (2002)
79. Wester, R., Davis, A.V., Bragg, A.E., Neumark, D.M.: Phys. Rev. A **65**, 051201 (2002)
80. Davis, A.V., Wester, R., Bragg, A.E., Neumark, D.M.: J. Chem. Phys. **119**, 2020 (2003)
81. Davis, A.V., Wester, R., Bragg, A.E., Neumark, D.M.: J. Chem. Phys. **118**, 999 (2003)
82. Wester, R., Bragg, A.E., Davis, A.V., Neumark, D.M.: J. Chem. Phys. **119**, 10032 (2003)
83. Zanni, M.T., Greenblatt, B.J., Davis, A.V., Neumark, D.M.: J. Chem. Phys. **111**, 2991 (1999)
84. Zanni, M.T., Frischkorn, C., Davis, A.V., Neumark, D.M.: J. Phys. Chem. A **104**, 2527 (2000)
85. Faeder, J., Parson, R.: J. Chem. Phys. **108**, 3909 (1998)
86. Batista, V.S., Zanni, M.T., Greenblatt, B.J., Neumark, D.M., Miller, W.H.: J. Chem. Phys. **110**, 3736 (1999)
87. Yu, N., Margulis, C.J., Coker, D.F.: J. Chem. Phys. **120**, 3657 (2004)

88. Miao, X.-Y., Wang, L., Yao, L., Song, H.-S.: Chem. Phys. Lett. **433**, 28 (2006)
89. Mabbs, R., Pichugin, K., Surber, E., Sanov, A.: J. Chem. Phys. **121**, 265 (2004)
90. Mabbs, R., Pichugin, K., Sanov, A.: J. Chem. Phys. **122**, 174305 (2005)
91. Gerhardt, P., Niemietz, M., Dok Kim, Y., Ganteför, G.: Chem. Phys. Lett. **382**, 454 (2003)
92. Heinzelmann, J., Kruppa, P., Proch, S., Kim, Y.D., Ganteför, G.: Chem. Phys. Lett. **603**, 1 (2014)
93. Lüttgens, G., Pontius, N., Bechthold, P.S., Neeb, M., Eberhardt, W.: Phys. Rev. Lett. **88**, 076102 (2002)
94. Kim, Y.D., Niemietz, M., Gerhardt, P, Gynz-Rekowski, F.V., Ganteför, G.: Phys. Rev. B **70**, 035421 (2004)
95. Niemietz, M., Koyasu, K., Ganteför, G., Kim, Y.D.: Chem. Phys. Lett. **438**, 263 (2007)
96. Koyasu, K., Niemietz, M., Götz, M., Ganteför, G.: Chem. Phys. Lett. **450**, 96 (2007)
97. Niemietz, M., Engelke, M., Kim, Y.D., Ganteför, G.: Appl. Phys. A **87**, 615 (2007)
98. Koyasu, K., Westhäuser, W., Niemietz, M., Heinen, J., Ganteför, G.: Appl. Phys. A **96**, 679 (2009)
99. Weber, J.M., Kim, J., Woronowicz, E.A., Weddle, G.H., Becker, I., Cheshnovsky, O., Johnson, M.A.: Chem. Phys. Lett. **339**, 337 (2001)
100. Bragg, A.E., Verlet, J.R.R., Kammrath, A., Cheshnovsky, O., Neumark, D.M.: Science **306**, 669 (2004)
101. Verlet, J.R.R., Bragg, A.E., Kammrath, A., Cheshnovsky, O., Neumark, D.M.: Science **307**, 93 (2005)
102. Bragg, A.E., Verlet, J.R.R., Kammrath, A., Cheshnovsky, O., Neumark, D.M.: J. Am. Chem. Soc. **127**, 15283 (2005)
103. Griffin, G.B., Young, R.M., Ehrler, O.T., Neumark, D.M.: J. Chem. Phys. **131**, 194302 (2009)
104. Young, R.M., Yandell, M.A., King, S.B., Neumark, D.M.: J. Chem. Phys. **136**, 094304 (2012)
105. Schwartz, B.J., Rossky, P.J.: J. Chem. Phys. **101**, 6902 (1994)
106. Schwartz, B.J., Rossky, P.J.: J. Chem. Phys. **101**, 6917 (1994)
107. Kimura, Y., Alfano, J.C., Walhout, P.K., Barbara, P.F.: J. Phys. Chem. **98**, 3450 (1994)
108. Kammrath, A., Verlet, J.R.R., Griffin, G.B., Neumark, D.M.: J. Chem. Phys. **125**, 076101 (2006)
109. Elkins, M.H., Williams, H.L., Neumark, D.M.: J. Chem. Phys. **144**, 184503 (2016)
110. Elkins, M.H., Williams, H.L., Shreve, A.T., Neumark, D.M.: Science **342**, 1496 (2013)
111. Karashima, S., Yamamoto, Y.-I., Suzuki, T.: Phys. Rev. Lett. **116**, 137601 (2016)
112. Lehr, L., Zanni, M.T., Frischkorn, C., Weinkauf, R., Neumark, D.M.: Science **284**, 635 (1999)
113. Kammrath, A., Verlet, J.R.R., Bragg, A.E., Griffin, G.B., Neumark, D.M.: J. Phys. Chem. A **109**, 11475 (2005)
114. Verlet, J.R.R., Kammrath, A., Griffin, G.B., Neumark, D.M.: J. Chem. Phys. **123**, 231102 (2005)
115. Turi, L., Sheu, W.-S., Rossky, P.J.: Science **309**, 914 (2005)
116. Madarász, Á., Rossky, P.J., Turi, L.: J. Chem. Phys. **130**, 124319 (2009)
117. Kammrath, A., Verlet, J.R.R., Griffin, G.B., Neumark, D.M.: J. Chem. Phys. **125**, 171102 (2006)
118. Kammrath, A., Griffin, G.B., Verlet, J.R.R., Young, R.M., Neumark, D.M.: J. Chem. Phys. **126**, 244306 (2007)
119. Young, R.M., Yandell, M.A., Neumark, D.M.: J. Chem. Phys. **134**, 124311 (2011)
120. Yandell, M.A., Young, R.M., King, S.B., Neumark, D.M.: J. Phys. Chem. A **116**, 2750 (2012)
121. Frischkorn, C., Zanni, M.T., Davis, A.V., Neumark, D.M.: Faraday Discuss. **115**, 49 (2000)
122. Lee, I.R., Lee, W., Zewail, A.H.: Chem. Phys. Chem. **9**, 83 (2008)
123. Ehrler, O.T., Griffin, G.B., Young, R.M., Neumark, D.M.: J. Phys. Chem. B **113**, 4031 (2009)
124. Young, R.M., Griffin, G.B., Kammrath, A., Ehrler, O.T., Neumark, D.M.: Chem. Phys. Lett. **485**, 59 (2010)
125. Young, R.M., Yandell, M.A., Niemeyer, M., Neumark, D.M.: J. Chem. Phys. **133**, 154312 (2010)

126. Young, R.M., Azar, R.J., Yandell, M.A., King, S.B., Head-Gordon, M., Neumark, D.M.: Mol. Phys. **110**, 1787 (2012)
127. Simons, J.: J. Phys. Chem. A **112**, 6401 (2008)
128. Bezchastnov, V.G., Vysotskiy, V.P., Cederbaum, L.S.: Phys. Rev. Lett. **107**, 133401 (2011)
129. Voora, V.K., Cederbaum, L.S., Jordan, K.D.: J. Phys. Chem. Lett. **4**, 849 (2013)
130. Klaiman, S., Gromov, E.V., Cederbaum, L.S.: J. Phys. Chem. Lett. **4**, 3319 (2013)
131. Voora, V.K., Jordan, K.D.: J. Phys. Chem. A **118**, 7201 (2014)
132. Klaiman, S., Gromov, E.V., Cederbaum, L.S.: Phys. Chem. Chem. Phys. **16**, 13287 (2014)
133. Voora, V.K., Jordan, K.D.: J. Phys. Chem. Lett. **6**, 3994 (2015)
134. Winghart, M.-O., Yang, J.-P., Vonderach, M., Unterreiner, A.-N., Huang, D.-L., Wang, L.-S., Kruppa, S., Riehn, C., Kappes, M.M.: J. Chem. Phys. **144**, 054305 (2016)
135. Rensing, C., Ehrler, O.T., Yang, J.-P., Unterreiner, A.-N., Kappes, M.M.: J. Chem. Phys. **130**, 234306 (2009)
136. Horke, D.A., Chatterley, A.S., Verlet, J.R.R.: J. Phys. Chem. Lett. **3**, 834 (2012)
137. Horke, D.A., Chatterley, A.S., Verlet, J.R.R.: Phys. Rev. Lett. **108**, 083003 (2012)
138. Chatterley, A.S., Horke, D.A., Verlet, J.R.R.: Phys. Chem. Chem. Phys. **14**, 16155 (2012)
139. Roberts, G.M., Lecointre, J., Horke, D.A., Verlet, J.R.R.: Phys. Chem. Chem. Phys. **12**, 6226 (2010)
140. Lecointre, J., Roberts, G.M., Horke, D.A., Verlet, J.R.R.: J. Phys. Chem. A **114**, 11216 (2010)
141. Horke, D.A., Roberts, G.M., Verlet, J.R.R.: J. Phys. Chem. A **115**, 8369 (2011)
142. Horke, D.A., Verlet, J.R.R.: Phys. Chem. Chem. Phys. **13**, 19546 (2011)
143. Bull, J.N., West, C.W., Verlet, J.R.R.: Phys. Chem. Chem. Phys. **17**, 16125 (2015)
144. Bull, J.N., West, C.W., Verlet, J.R.R.: Chem. Sci. **7**, 5352 (2016)
145. Bull, J.N., West, C.W., Verlet, J.R.R.: Chem. Sci. **6**, 1578 (2015)
146. Lee, I.R., Bañares, L., Zewail, A.H.: J. Am. Chem. Soc. **130**, 6708 (2008)
147. Horke, D.A., Verlet, J.R.R.: Phys. Chem. Chem. Phys. **14**, 8511 (2012)
148. West, C.W., Hudson, A.S., Cobb, S.L., Verlet, J.R.R.: J. Chem. Phys. **139**, 071104 (2013)
149. West, C.W., Bull, J.N., Hudson, A.S., Cobb, S.L., Verlet, J.R.R.: J. Phys. Chem. B **119**, 3982 (2015)
150. Ullrich, S., Schultz, T., Zgierski, M.Z., Stolow, A.: J. Am. Chem. Soc. **126**, 2262 (2004)
151. Chatterley, A.S., West, C.W., Roberts, G.M., Stavros, V.G., Verlet, J.R.R.: J. Phys. Chem. Lett. **5**, 843 (2014)
152. Yandell, M.A., King, S.B., Neumark, D.M.: J. Am. Chem. Soc. **135**, 2128 (2013)
153. King, S.B., Yandell, M.A., Neumark, D.M.: Faraday Discuss. **163**, 59 (2013)
154. King, S.B., Yandell, M.A., Stephansen, A.B., Neumark, D.M.: J. Chem. Phys. **141**, 224310 (2014)
155. Li, W.-L., Kunin, A., Matthews, E., Yoshikawa, N., Dessent, C.E.H., Neumark, D.M.: J. Chem. Phys. **145**, 044319 (2016)
156. King, S.B., Stephansen, A.B., Yokoi, Y., Yandell, M.A., Kunin, A., Takayanagi, T., Neumark, D.M.: J. Chem. Phys. **143**, 024312 (2015)
157. Kunin, A., Li, W.-L., Neumark, D.M.: J. Chem. Phys. **149**, 084301 (2018)
158. Stephansen, A.B., King, S.B., Yokoi, Y., Minoshima, Y., Li, W.-L., Kunin, A., Takayanagi, T., Neumark, D.M.: J. Chem. Phys. **143**, 104308 (2015)
159. Kunin, A., Li, W.-L., Neumark, D.M.: Phys. Chem. Chem. Phys. **18**, 33226 (2016)
160. Barrios, R., Skurski, P., Simons, J.: J. Phys. Chem. B **106**, 7991 (2002)
161. Simons, J.: Acc. Chem. Res. **39**, 772 (2006)
162. Chen, H.-Y., Yang, P.-Y., Chen, H.-F., Kao, C.-L., Liao, L.-W.: J. Phys. Chem. B **118**, 11137 (2014)
163. Berdys, J., Anusiewicz, I., Skurski, P., Simons, J.: J. Am. Chem. Soc. **126**, 6441 (2004)
164. Berdys, J., Skurski, P., Simons, J.: J. Phys. Chem. B **108**, 5800 (2004)
165. Alizadeh, E., Sanche, L.: Chem. Rev. **112**, 5578 (2012)
166. Bachorz, R.A., Klopper, W., Gutowski, M., Li, X., Bowen, K.H.: J. Chem. Phys. **129**, 054309 (2008)
167. Desfrançois, C., Abdoul-Carime, H., Schermann, J.-P.: Int. J. Mod. Phys. B **10**, 1339 (1996)

168. Crawford, O.H.: Mol. Phys. **20**, 585 (1971)
169. Kulakowska, I., Geller, M., Lesyng, B., Wierzchowski, K.L.: Biochimica et Biophys. Acta (BBA) Nucleic Acids Protein Synth. **361**, 119 (1974)
170. Carles, S., Lecomte, F., Schermann, J.P., Desfrançois, C.: J. Phys. Chem. A **104**, 10662 (2000)
171. Hanus, M., Kabelac, M., Rejnek, J., Ryjacek, F., Hobza, P.: J. Phys. Chem. B **108**, 2087 (2004)
172. Burrow, P.D., Gallup, G.A., Scheer, A.M., Denifl, S., Ptasińska, S., Märk, T.D., Scheier, P.: J. Chem. Phys. **124**, 124310 (2006)
173. Hanel, G., Gstir, B., Denifl, S., Scheier, P., Probst, M., Farizon, B., Farizon, M., Illenberger, E., Märk, T.D.: Phys. Rev. Lett. **90**, 188104 (2003)
174. Ptasińska, S., Denifl, S., Gohlke, S., Scheier, P., Illenberger, E., Märk, T.D.: Angew. Chem. Int. Ed. **45**, 1893 (2006)
175. Denifl, S., Ptasinska, S., Hanel, G., Gstir, B., Probst, M., Scheier, P., Mark, T.D.: J. Chem. Phys. **120**, 6557 (2004)
176. Denifl, S., Sulzer, P., Zappa, F., Moser, S., Kraeutler, B., Echt, O., Bohme, D.K., Maerk, T.D., Scheier, P.: Int. J. Mass Spectrom. **277**, 296 (2008)
177. Gallup, G.A., Fabrikant, I.I.: Phys. Rev. A **83**, 012706 (2011)
178. Hendricks, J.H., Lyapustina, S.A., de Clercq, H.L., Snodgrass, J.T., Bowen, K.H.: J. Chem. Phys. **104**, 7788 (1996)
179. Schiedt, J., Weinkauf, R., Neumark, D.M., Schlag, E.W.: Chem. Phys. **239**, 511 (1998)
180. Sommerfeld, T.: J. Phys. Chem. A **108**, 9150 (2004)
181. Takayanagi, T., Asakura, T., Motegi, H.: J. Phys. Chem. A **113**, 4795 (2009)
182. Motegi, H., Takayanagi, T.: J. Mol. Struct. (Thoechem) **907**, 85 (2009)
183. Yokoi, Y., Kano, K., Minoshima, Y., Takayanagi, T.: Comput. Theor. Chem. **1046**, 99 (2014)
184. Gu, J., Leszczynski, J., Schaefer, H.F.: Chem. Rev. **112**, 5603 (2012)
185. Compton, R.N., Carman, H.S., Desfrancois, C., Abdoulcarmine, H., Schermann, J.P., Hendricks, J.H., Lyapustina, S.A., Bowen, K.H.: J. Chem. Phys. **105**, 3472 (1996)
186. Bachorz, R.A., Klopper, W., Gutowski, M.: J. Chem. Phys. **126**, 085101 (2007)
187. Desfrancois, C., AbdoulCarime, H., Schermann, J.P.: J. Chem. Phys. **104**, 7792 (1996)
188. Dolgounitcheva, O., Zakrzewski, V.G., Ortiz, J.V.: Chem. Phys. Lett. **307**, 220 (1999)
189. Dolgounitcheva, O., Zakrzewski, V.G., Ortiz, J.V.: J. Phys. Chem. A **105**, 8782 (2001)
190. Svozil, D., Frigato, T., Havlas, Z., Jungwirth, P.: Phys. Chem. Chem. Phys. **7**, 840 (2005)
191. Hendricks, J.H., Lyapustina, S.A., de Clercq, H.L., Bowen, K.H.: J. Chem. Phys. **108**, 1 (1998)
192. Matthews, E., Cercola, R., Mensa-Bonsu, G., Neumark, D.M., Dessent, C.E.H.: J. Chem. Phys. **148**, 084304 (2018)
193. Middleton, C.T., de La Harpe, K., Su, C., Law, Y.K., Crespo-Hernández, C.E., Kohler, B.: Annu. Rev. Phys. Chem. **60**, 217 (2009)
194. Kleinermanns, K., Nachtigallová, D., de Vries, M.S.: Int. Rev. Phys. Chem. **32**, 308 (2013)
195. Improta, R., Santoro, F., Blancafort, L.: Chem. Rev. **116**, 3540 (2016)
196. Peláez, R.J., Blondel, C., Delsart, C., Drag, C.: J. Phys. B-At. Mol. Opt. **42**, 125001 (2009)
197. Wiley, W.C., McLaren, I.H.: Rev. Sci. Instrum. **26**, 1150 (1955)
198. Eppink, A., Parker, D.H.: Rev. Sci. Instrum. **68**, 3477 (1997)
199. Dribinski, V., Ossadtchi, A., Mandelshtam, V., Reisler, H.: Rev. Sci. Instrum. **73**, 2634 (2002)
200. Frisch, M.J., Trucks, G.W., Schlegel, H.B., Scuseria, G.E., Robb, M.A., Cheeseman, J.R., Scalmani, G., Barone, V., Mennucci, B., Petersson, G.A., Nakatsuji, H., Caricato, M., Li, X., Hratchian, H.P., Izmaylov, A.F., Bloino, J., Zheng, G., Sonnenberg, J.L., Hada, M., Ehara, M., Toyota, K., Fukuda, R., Hasegawa, J., Ishida, M., Nakajima, T., Honda, Y., Kitao, O., Nakai, H., Vreven, T., Montgomery Jr., J.A., Peralta, J.E., Ogliaro, F., Bearpark, M.J., Heyd, J., Brothers, E.N., Kudin, K.N., Staroverov, V.N., Kobayashi, R., Normand, J., Raghavachari, K., Rendell, A.P., Burant, J.C., Iyengar, S.S., Tomasi, J., Cossi, M., Rega, N., Millam, N.J., Klene, M., Knox, J.E., Cross, J.B., Bakken, V., Adamo, C., Jaramillo, J., Gomperts, R., Stratmann, R.E., Yazyev, O., Austin, A.J., Cammi, R., Pomelli, C., Ochterski, J.W., Martin, R.L., Morokuma, K., Zakrzewski, V.G., Voth, G.A., Salvador, P., Dannenberg, J.J., Dapprich, S., Daniels, A.D., Farkas, Ö., Foresman, J.B., Ortiz, J.V., Cioslowski, J., Fox, D.J. Gaussian, Inc., Wallingford, CT, USA (2009)

201. Dessent, C.E.H., Kim, J., Johnson, M.A.: Faraday Discuss. **115**, 395 (2000)
202. Lecomte, F., Carles, S., Desfrançois, C., Johnson, M.A.: J. Chem. Phys. **113**, 10973 (2000)
203. Adams, C.L., Schneider, H., Ervin, K.M., Weber, J.M.: J. Chem. Phys. **130**, 074307 (2009)
204. Sansonetti, J.E., Martin, W.C.: J. Phys. Chem. Ref. Data **34**, 1559 (2005)
205. Metz, R.B., Cyr, D.R., Neumark, D.M.: J. Phys. Chem. **95**, 2900 (1991)
206. Beyer, T., Swinehart, D.F.: Commun. ACM **16**, 379 (1973)
207. Stein, S.E., Rabinovitch, B.S.: J. Chem. Phys. **58**, 2438 (1973)
208. Hase, W.L.: Science **266**, 998 (1994)
209. Wang, H., Peslherbe, G.H., Hase, W.L.: J. Am. Chem. Soc. **116**, 9644 (1994)
210. Peslherbe, G.H., Wang, H., Hase, W.L.: J. Chem. Phys. **102**, 5626 (1995)
211. Chabinyc, M.L., Craig, S.L., Regan, C.K., Brauman, J.I.: Science **279**, 1882 (1998)
212. Xie, J., Otto, R., Mikosch, J., Zhang, J., Wester, R., Hase, W.L.: Acc. Chem. Res. **47**, 2960 (2014)
213. Simons, J.: J. Am. Chem. Soc. **103**, 3971 (1981)
214. Acharya, P.K., Kendall, R.A., Simons, J.: J. Am. Chem. Soc. **106**, 3402 (1984)
215. Campbell, E.E.B., Levine, R.D.: Annu. Rev. Phys. Chem. **51**, 65 (2000)
216. Andersen, J.U., Bonderup, E., Hansen, K.: Journal of Physics B: Atomic. Mol. Opt. Phys. **35**, R1 (2002)
217. Mazurkiewicz, K., Bachorz, R.A., Gutowski, M., Rak, J.: J. Phys. Chem. B **110**, 24696 (2006)
218. Oyler, N.A., Adamowicz, L.: J. Phys. Chem. **97**, 11122 (1993)
219. Liu, H.-T., Ning, C.-G., Huang, D.-L., Wang, L.-S.: Angew. Chem. Int. Edit. **53**, 2464 (2014)
220. Parsons, B.F., Sheehan, S.M., Yen, T.A., Neumark, D.M., Wehres, N., Weinkauf, R.: Phys. Chem. Chem. Phys. **9**, 3291 (2007)
221. Williams, H.L., Erickson, B.A., Neumark, D.M.: J. Chem. Phys. **148**, 194303 (2018)
222. Buchner, F., Ritze, H.H., Lahl, J., Lubcke, A.: Phys. Chem. Chem. Phys. **15**, 11402 (2013)
223. Buchner, F., Nakayama, A., Yamazaki, S., Ritze, H.H., Lubcke, A.: J. Am. Chem. Soc. **137**, 2931 (2015)